Journal of Molecular Catalysis B: Enzymatic 66 (2010) 90–94

Contents lists available at ScienceDirect

Journal of Molecular Catalysis B: Enzymatic

journal homepage: www.elsevier.com/locate/molcatb

Enantioselective hydrolysis of diethyl 3-hydroxyglutarate to ethyl (*S*)-3-hydroxyglutarate by immobilized *Candida antarctica* lipase B

Hua-Ping Dong, Ya-Jun Wang, Yu-Guo Zheng*

Institute of Bioengineering, Zhejiang University of Technology, Hangzhou, Zhejiang Province 310014, PR China

ARTICLE INFO

Article history:
Received 31 October 2009
Received in revised form 20 March 2010
Accepted 20 March 2010
Available online 27 March 2010

Keywords:
Ethyl (S)-3-hydroxyglutarate
Enantioselective hydrolysis
Uncompetitive inhibition
Enantioselectivity
Kinetic constants

ABSTRACT

Optically pure ethyl (*S*)-3-hydroxyglutarate [(*S*)-3-EHG] is used as a key precursor for synthesis of a variety of pharmaceutically important compounds. In this work, we established an efficient procedure for enantioselectively hydrolyzing diethyl 3-hydroxyglutarate (3-DHG) to optically active (*S*)-3-EHG employing immobilized *Candida antarctica* lipase B (Novozym 435). Under the optimized conditions: pH 7.0, agitation speed 200 rpm, temperature 40 °C, 3-DHG concentration 0.15 mol L^{-1}, and enzyme loading 7 g L^{-1}, (*S*)-3-EHG was prepared in above 95% *ee* value and 98.5% yield, and the reaction was free from external mass transfer and intra-particle diffusion limitations and kinetically controlled. The inhibitions of substrate (3-DHG) and product (3-EHG) were excluded because both displayed no decline in activity at elevated concentrations within the given ranges. In addition, ethanol, a byproduct of the reaction, inhibited lipase B following an uncompetitive inhibition pattern. The kinetic constants were obtained through non-linear regression, with values of V_{max} 1.29 mmol min^{-1} g^{-1}, K_m 0.06 mol L^{-1}, and K_i 0.37 mol L^{-1}, respectively.

1. Introduction

Optically active ethyl 3-hydroxyglutarate [3-EHG] is an attractive building block for synthesis of a variety of pharmaceutically important compounds, such as statins, pimaricin and L-carnitine [1–6]. Ethyl (*S*)-3-hydroxyglutarate [(*S*)-3-EHG] is a precursor to various enantiopure intermediates for chiral drugs including cholesterol-lowering drugs like Lipitor®, and L-carnitine which is a required vitamin analogue for mammalian metabolism and is applied in the active treatment of systemic and myopathic deficiencies [7–9]. The enantiopure compounds with *R*-configuration such as ethyl (*R*)-3-hydroxyglutarate (*ee* > 98%) and 4-cyano-(*R*)-3-hydroxybutanoate are synthesized by enzymatic catalysis [3,5,10,11]. By contrast, few reports concerning preparation of (*S*)-3-EHG through enantioselective hydrolysis of prochiral diethyl 3-hydroxyglutarate (3-DHG) are available [1,2]. Gopalan et al. prepared (*S*)-3-EHG with the yield and *ee* value of 38% and 69%, using *Arthrobacter* sp. (ATCC 19140). Thereafter, Jacobsen et al. provided a promising synthetic routine featured by improved *ee* value of 91% and yield of 80% employing immobilized *C. antarctica* lipase B (CALB, Novozym 435); and they also prepared 4-cyano-(*S*)-3-hydroxybutanoate in *ee* value of 98% from 4-carbamoyl-(*S*)-3-hydroxybutanoate [12]. The problem in existing (*S*)-3-EHG biosynthesis is that enantiopurities and the yields of these methods are not satisfactory, which failed to meet the requirement for enantiopure compound, and leaded to no commercial (*S*)-3-EHG available. In addition, there are no reports by far about the studies on the reaction kinetics and enzymatic mechanisms.

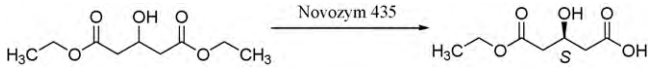

Scheme 1. Enantioselective hydrolysis of 3-DHG to (*S*)-3-EHG catalyzed by Novozym 435.

Candida antarctica lipase B exhibits excellent thermal stability, activity and stereospecificity [13,14], and is widely applied in organic synthesis for esterification and hydrolysis [13], displaying critical industrial importance. Its enzymatic performance can be further enhanced to various extents through immobilization onto a multitude of support materials, including hydrophilic or hydrophobic polymers [15–20].

In the present work, we attempted to establish an efficient bioconversion of 3-DHG to enantiopure (*S*)-3-EHG (Scheme 1) by commercial CALB (Novozym 435), and study the reaction kinetics in detail. Moreover, the operating parameters including reaction temperature, pH, and mass transfer limitations, as well as inhibitory effects of substrate and products on commercial CALB were examined.

* Corresponding author. Tel.: +86 571 88320379; fax: +86 571 88320630.
E-mail address: zhengyg@zjut.edu.cn (Y.-G. Zheng).

1381-1177/$ – see front matter © 2010 Elsevier B.V. All rights reserved.
doi:10.1016/j.molcatb.2010.03.009

2. Experimental

2.1. Enzyme and chemicals

Novozym 435 (CALB, fraction B of lipase from *C. antarctica* immobilized on macroporous polyacrylate resin, diameter varying between 0.3 mm and 0.9 mm) was supplied by Novozymes, Denmark. 3-DHG was purchased from Sigma. Other chemicals were of analytical grade. (*S*)-3-EHG (*ee* ≥ 95%) was prepared in our laboratory.

2.2. Hydrolytic reaction

The hydrolytic reaction was carried out in a 50 ml erlenmeyer flask in a shaking water bath tank at 40 °C and 200 rpm. 1.5 mmol of 3-DHG was dissolved into 10 ml sodium phosphate buffer (30 mmol L^{-1}, pH 7.0), and then 0.07 g Novozym 435 was added to initialize the reaction. During the reaction process for 30 min, pH value of reaction media was kept at 7.0 by titrating with a 1 N NaOH using a pH-Stat technique unless stated otherwise. At regular intervals, 0.5 ml aliquot sample was withdrawn to detect 3-DHG and (*S*)-3-EHG.

Otherwise, the enzyme was filtered off at the end of the reaction, and the filtrate was subjected to ethyl acetate extraction after pH adjusted to 2 with 2 N HCl. The extract phase was dehydrated by anhydrous Na_2SO_4, and ethyl acetate was removed by reduced distillation to obtain the product.

2.3. Determination of the product

The chemical structure of the product was determined by ^1H (500 MHz) and ^{13}C NMR (100 MHz) recorded with a NMR spectrometer (Bruker Avace III), using deuteriochloroform as the solvent. The stereoconfiguration of the product was determined by measurement of specific rotation of the product (Rudolf AutoPol IV, USA). The chemical purity (≥98%) was determined by HPLC, and *ee* value of the product was measured by normal phase HPLC after a derivative reaction with chiral amine [21].

The product was elucidated to be enantiopure (*S*)-3-EHG (*ee* ≥ 95%) based on the following experimental data. ^1H NMR (ppm): δ 1.28 (3H, t, J = 7.0 MHz), 2.59 (4H, dd), 4.18 (2H, q, J = 7.0 MHz), 4.49 (1H, m), ^{13}C NMR (ppm): δ 13.87, 40.32, 40.52, 60.83, 64.53, 171.82, 175.66. The specific rotation ($[\alpha]_D^{20}$) of +1.90 (c 11.5, in acetone) confirmed *S* configuration [1], and *ee* value was calculated to be ≥95%.

2.4. Determination of specific initial rate

Specific initial rate was defined as mmol of 3-EHG produced per minute and per gram of enzyme, and determined from the time course of 3-EHG formation using a second order polynomial fitting by regression analysis of 3-EHG concentration and determining the initial slope of the tangent to the curve.

2.5. High performance liquid chromatography (HPLC) analysis

The content of the substrate and product was determined and quantified by HPLC using a hypersil ODS 2 column (4.6 mm × 250 mm, 5 μm) at room temperature. The mobile phase consisted of acetonitrile and 0.5% (v/v) aqueous triethylamine solution at ratio of 1:4 (v/v). The flow rate was set at 1 ml min^{-1}; and the injection volume of each sample was 10 μl. By using a UV-detector (Spd-10 A Vp plus, Shimadzu), 3-DHG was monitored at 220 nm with retention time of 5.50 min; 3-EHG was detected at 260 nm with retention time of 4.10 min.

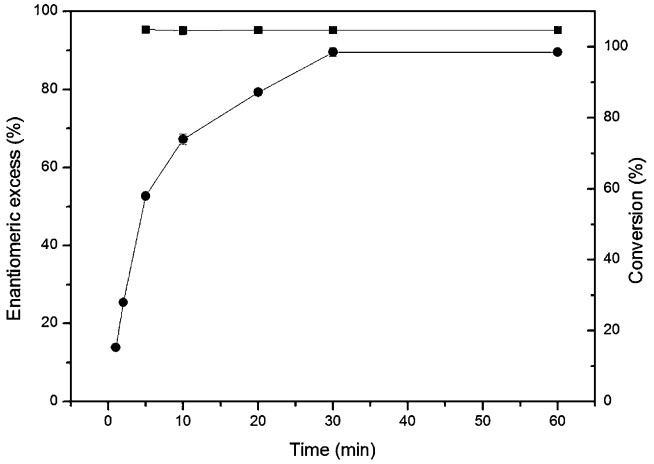

Fig. 1. Time evolution of total conversion (●) and *ee* value of (*S*)-3-EHG (■) at 3-DHG concentration of 0.15 mol L^{-1}. Operating conditions: 40 °C, pH 7.0, 200 rpm, and 0.07 g CALB.

2.6. ee Value of (S)-3-EHG determination

Determination of the *ee* value of (*S*)-3-EHG was based on a normal phase HPLC separation of (*R*)- and (*S*)-3-EHG after converting 3-EHG into two diastereomers by a derivative reaction with chiral amine [21]. The normal phase HPLC conditions were as follows: the mobile phase was petroleum ether–dichlormethane (1:10), and flow rate was set at 1.5 ml min^{-1}. The sample (20 μl) was loaded onto a silica gel column (Kromasil; 250 mm × 4.6 mm, 5 μm) and visualized under 254 nm UV light. The retention times of the derivatives of (*R*)-3-EHG (D-**1**) and (*S*)-3-EHG (D-**2**) were 3.85 min and 4.15 min, respectively. The *ee* values were obtained by the ratio of peak areas of D-**1** (A_1) and D-**2** (A_2) as follows: $ee\ (\%) = (A_2 - A_1)/(A_2 + A_1) \times 100$.

3. Results and discussion

3.1. 3-EHG synthesis procedure

3-DHG conversion profile was firstly investigated under controlled and uncontrolled pH conditions at 40 °C, catalyzed by Novozym 435. In the uncontrolled pH case, pH of reaction solution dropped sharply from 7.20 to 3.70, attributing to the accumulation of 3-EHG. Accordingly, the conversion of 3-DHG declined to 70% partly because of the inhibitory effect of acidified environments on Novozym 435. In contrast with the uncontrolled pH case, the conversion was elevated to be 98.5% at "regulated pH" of 7.0, showing that the pH control during the reaction was advantageous to keep high enzymatic activity. As shown in Fig. 1, the reaction rate was fast in the initial 5 min, possessing a linear correlation with reaction time; and it decreased with reduced substrate concentration. The *ee* value of (*S*)-3-EHG remained invariant at high value during the reaction process, and the conversion of the monoacids to diacids was also not observed, demonstrating that Novozym 435 possesses excellent regioselectivity and enantioselectivity.

3.2. Influence of mass transfer limitation on hydrolytic reaction

Due to two phases containing aqueous bulk and the solid bound enzyme in the reaction media, the influence of mass transfer in the external bulk and intra-particle should be properly assessed. The effect of the external mass transfer limitation could be solved by increasing the agitation speed. As shown in Fig. 2, the initial rate increased with agitation speed up to 200 rpm. No dependence of

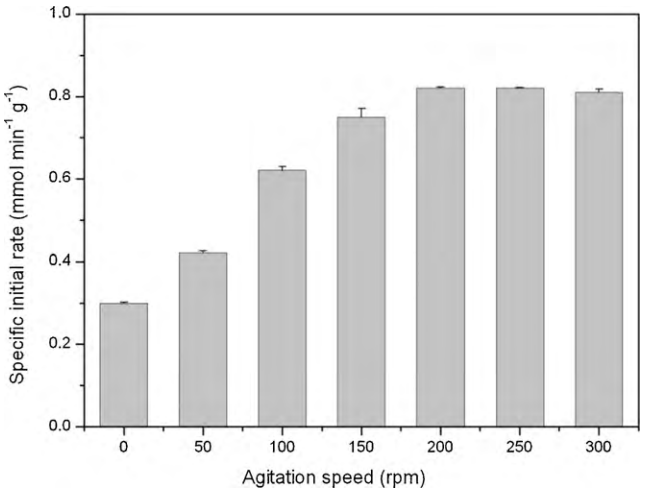

Fig. 2. Effect of agitation speed on specific initial rate. Operating conditions: 40 °C, pH 7.0, 0.07 g CALB, and 0.15 mol L^{-1} 3-DHG.

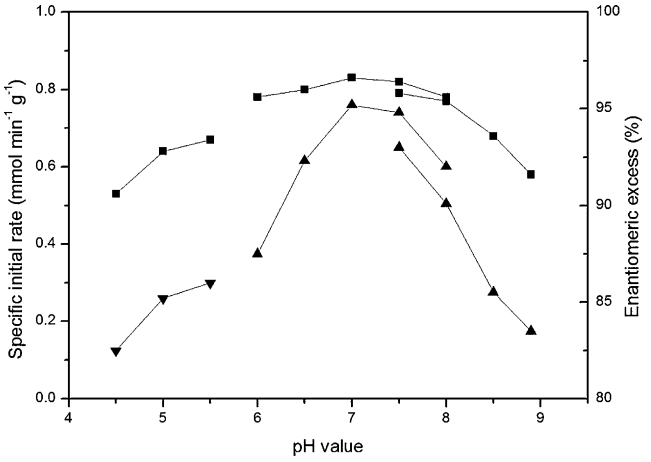

Fig. 3. Effect of pH on specific initial rate (■) and *ee* value (▲) of (*S*)-3-EHG. Operating conditions: 40 °C, 200 rpm, 0.07 g CALB, 0.15 mol L^{-1} 3-DHG, and pH value of reaction media was kept at the initial value. Sodium acetate buffer, 4.5–5.5; sodium phosphate buffer, 6.0–8.0; Tris–HCl buffer, 7.5–8.9.

initial rate on agitation speed over 200 rpm was observed, suggesting that no external diffusion limitation was present at that speed. Therefore, the agitation speed was set at 200 rpm to remove the external mass transfer limitation.

Intra-particle diffusion resistance was confirmed by calculating Thiele's modulus, Φ, which is given as [22]:

$$\Phi = \frac{v}{D_E C}\left(\frac{V_P}{A_P}\right)^2 \quad (1)$$

where v is the reaction rate (mmol s^{-1}g^{-1}), D_E is the effective diffusivity coefficient (cm^2 s^{-1}), C is the substrate concentration (mol L^{-1}), V_P is Novozym 435 particle volume (cm^3), and A_P is the surface area of the Novozym 435 particle (cm^2). Since the enzyme particle is spherical, Thiele's modulus can be expressed as:

$$\Phi = \frac{v}{D_E C}\left(\frac{R}{3}\right)^2 \quad (2)$$

and D_E expression can be given as:

$$D_E = D_S\frac{\varepsilon}{\tau} \quad (3)$$

where ε is the porosity of the particle, τ is the tortuosity factor of the particle, and D_S is the substrate diffusivity in the reaction medium (cm^2 s^{-1}). D_S could be estimated to be 5.89×10^{-5} cm^2 s^{-1} from the Siebel equation [23]. In addition, the values of ε and τ were 0.5 and 6, respectively, so the value of D_E was calculated to be 4.91×10^{-6} from Eq. (3). By substituting the appropriate values into Eq. (2), with $v = 0.022$ mmol s^{-1} g^{-1} (maximum reaction rate), $C = 0.15$ mol L^{-1}, $R = 0.03$ cm, and $D_E = 4.91 \times 10^{-6}$ cm^2 s^{-1}, Φ was calculated to be 0.003. Such a small value for Thiele's modulus indicated that the reaction was kinetically controlled and the intra-particle diffusion could be neglected, which may be attributed to the small particle size and comparatively large pore size of Novozym 435.

3.3. Effect of pH

Enzymes are catalysts with a high dependence on pH. Generally, they have an optimal working pH, and higher or lower values can lead to partial inactivation. Extreme pH can disrupt enzyme tertiary structure and result in catalytic activity loss. Different buffer solutions with pH varying from 4.5 to 9.0 were chosen, and the pH value for each treatment was kept constant during the reaction process using a pH-Stat technique. As shown in Fig. 3, Novozym 435 showed higher activity in the range from pH 6.0 to 8.0, and declined to different extents beyond this range. On the other hand, the optimum pH for the enantioselectivity was located at between 7.0 and 7.5; besides, the declining trend in *ee* values outside the optimal pH range was strikingly more pronounced than that of yields, suggesting that the enantioselectivity was more vulnerable to pH changes. Due to the best activity and enantioselectivity of Novozym 435 at pH 7.0, the hydrolytic reaction was suitably to be performed in the neutral media.

3.4. Effect of temperature

The thermal stability of biocatalysts is always taken as one of the most important criteria for industrial applications. Novozym 435 is regarded as being rather resistant to heat, so the examined temperature range was broadened from 20 to 70 °C in the present work. The maximum values of the activity and enantioselectivity were commonly observed at 40 °C (Fig. 4). The enzymatic activity improved with temperatures from 20 °C to 40 °C, and the enzyme was still very active at 50 °C. However, the higher enantioselectivity was maintained at temperatures below 40 °C, and it decreased sharply at temperatures exceeding 40 °C, demonstrating that the excessive high temperature resulted in the conformational change of the active site, which determines the enantioselectivity of Novozym 435. In addition, within the temperature range from

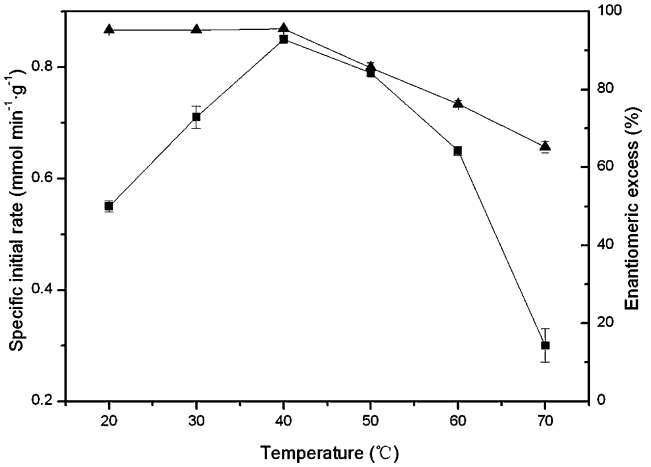

Fig. 4. Effect of temperature on specific initial rate (■) and *ee* value (▲) of (*S*)-3-EHG. Operating conditions: 200 rpm, pH 7.0, 0.07 g CALB, and 0.15 mol L^{-1} 3-DHG.

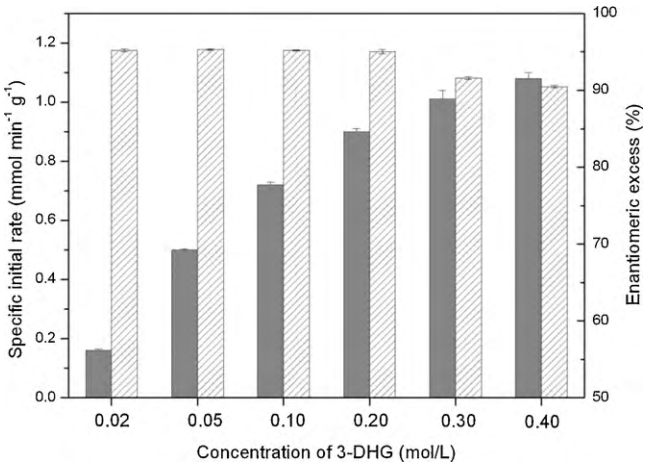

Fig. 5. Effect of 3-DHG concentration on specific initial rate (■) and *ee* value (▨) of (*S*)-3-EHG. Operating conditions: 40 °C, 200 rpm, pH 7.0, and 0.07 g CALB.

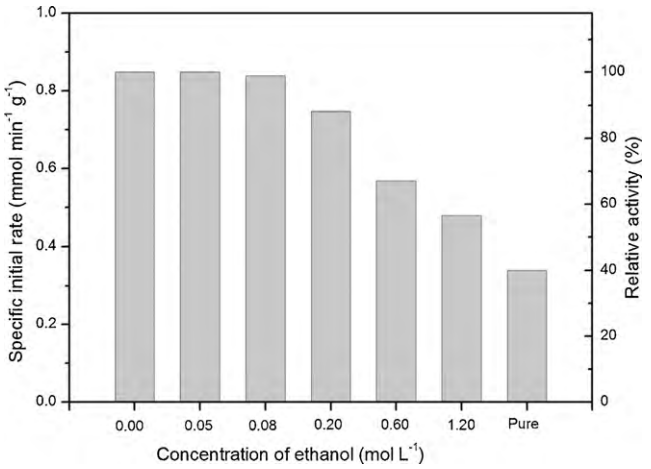

Fig. 6. Effect of initial ethanol concentration on specific initial rate. Operating conditions: 40 °C, 200 rpm, pH 7.0, 0.07 g CALB, and 0.15 mol L^{-1} 3-DHG.

20 °C to 40 °C, the hydrolytic reaction catalyzed by Novozym 435 obeyed Arrhenius law, and the activation energy, E_a, was calculated to be 16.63 kJ mol^{-1}.

3.5. Determination of substrate inhibition

It was observed in Fig. 5 that the reaction rate increased with the elevated amounts of 3-DHG up to 0.40 mol L^{-1}, suggesting that more 3-DHG molecules were available to bind the active sites of the enzyme as the amount of 3-DHG increasing, and 3-DHG had no inhibitory effect on enzyme activity. On the contrary, *ee* value of (*S*)-3-EHG decreased with 3-DHG concentration exceeding 0.2 mol L^{-1}. This was consistent with the finding of Jacobsen et al. that *ee* value of (*S*)-3-EHG dropped from 90% to 87% as 3-DHG increased from 0.30 mol L^{-1} to above 1 mol L^{-1} [1]. Such negative effect on enantioselectivity was probably resulted from the strengthened hydrophobic interaction between excessive 3-DHG and Novozym 435 [17], which leaded to the conformational change in the active site of Novozym 435 [24]. Therefore, lowering 3-DHG concentration was advantageous to raise *ee* value of (*S*)-3-EHG, and the similar dependence of enantioselectivity of biocatalyst on the substrate concentration was also found in the nitrilase-catalyzed hydrolytic reaction [25].

3.6. Determination of product inhibition

Enzymes do not alter reaction equilibrium because they do not affect thermodynamics; increasing the product concentration always speeds up reverse reaction, yielding apparent product inhibition. 3-EHG and ethanol were produced in the hydrolysis of 3-DHG. Addition of 3-EHG into the solution before reaction would cause pH drop, which was proved to result in decreases in the activity and enantioselectivity of Novozym 435. To exclude pH fluctuation and effect thereof, pH of reaction media were maintained at 7.0 with 1 N NaOH. Under this condition, the conversions (>98%) and *ee* values (≥95%) almost remained invariant as the initial 3-EHG concentration increased up to 0.2 mol L^{-1}, indicating it was the acidified conditions caused by 3-EHG accumulation, not 3-EHG itself, that inhibited Novozym 435.

However, 60% of enzymatic activity was lost when nearly pure alcohol (containing 3% water as the substrate) was used as the reaction media, suggesting that the activity was not totally lost as Novozym 435 was exposed to the pure alcohol because of its good tolerance to the organic phase. The details about inhibition of byproduct ethanol on Novozym 435 at concentrations above 0.08 mol L^{-1} was shown in Fig. 6.

3.7. Kinetics and mechanism of reaction

Generally, hydrolytic reactions performed in an aqueous solution conform to uni-bi kinetic mechanisms, because water is present in large quantities and the variation in its concentration is negligible. In the case of ethanol inhibition, the dissociation constant K_i should be included in the kinetic model. Therefore, the equations for different inhibitions are described below:

Competitive inhibition,

$$v = \frac{V_{max}[S]}{K_m(1 + [I]/K_i) + [S]} \quad (4)$$

Noncompetitive inhibition,

$$v = \frac{V_{max}[S]}{K_m(1 + [I]/K_i) + [S](1 + [I]/K_i)} \quad (5)$$

Uncompetitive inhibition,

$$v = \frac{V_{max}[S]}{K_m + [S](1 + [I]/K_i)} \quad (6)$$

where v is the apparent initial reaction rate, V_{max} is the apparent maximum reaction rate, [S] is the substrate (3-DHG) concentration, [I] is the initial ethanol concentration, K_m is the Michaelis–Menten constant, and K_i is the dissociation constant of ethanol binding to lipase–substrate complex.

In order to validate the kinetic mechanism, the inhibition plot was generated by measuring the initial reaction rate at varying 3-DHG concentrations at each fixed concentration of ethanol (0–0.4 mol L^{-1}). As shown in Fig. 7, the Lineweaver–Burk plots of velocities versus 3-DHG concentrations at different fixed ethanol concentrations yielded a set of lines with the same slope, indicating a typical uncompetitive inhibition. This result was further confirmed by non-linear fitting of the data to the uncompetitive model (Eq. (6)). In other words, ethanol could not bind to the free lipase, but bind to the bound forms of enzyme and 3-DHG, forming a non-productive end complex. The maximum reaction velocity (V_{max}), Michaelis constant (K_m) and inhibition constant (K_i) were calculated to be 1.29 mmol min^{-1} g^{-1}, 0.06 mol L^{-1} and 0.37 mol L^{-1} through non-linear regression analysis. The obtained parameters were used to simulate initial rate versus concentration of 3-DHG at 0.2 mol L^{-1} ethanol. Fig. 8 showed that the experimental model fitted the data very well.

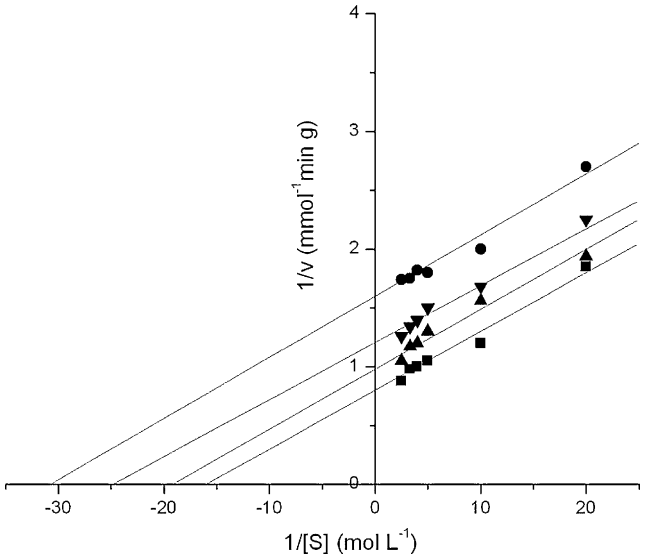

Fig. 7. Lineweaver–Burk plot of reciprocal initial rates versus reciprocal 3-DHG concentration at different ethanol concentrations. (■) 0 mol L^{-1}, (▲) 0.1 mol L^{-1}, (▼) 0.2 mol L^{-1}, (●) 0.4 mol L^{-1}. Operating conditions: 40 °C, 200 rpm, pH 7.0, and 0.07 g CALB.

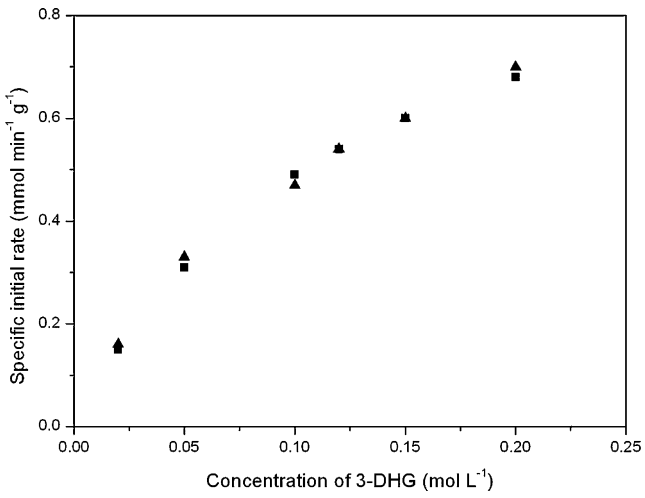

Fig. 8. Comparison of simulated (■) and experimental initial rates (▲) versus concentration of 3-DHG. Operating conditions: 40 °C, 200 rpm, pH 7.0, 0.07 g CALB, and 0.2 mol L^{-1} ethanol.

4. Conclusion

The detailed investigation of reaction kinetics and enzymatic mechanisms in enantioselective hydrolysis of 3-DHG was firstly conducted in this study, in addition to optimization of reaction conditions, especially the agitation speed, pH, temperature and concentration of 3-DHG, which were key factors influencing the yield and *ee* value of (*S*)-3-EHG. Under the optimized reaction conditions: pH 7.0, agitation speed 200 rpm, temperature 40 °C, substrate concentration 0.15 mol L^{-1}, and the enzyme loading 7 g L^{-1}, (*S*)-3-EHG with *ee* value above 95% was obtained by Novozym 435 catalysis, and the conversion reached above 98%. Both values were much improved in comparison with the previous study.

In addition, the absence of internal diffusion limitation in the immobilized particle in this hydrolytic reaction was confirmed. It was also explained that 3-DHG and 3-EHG had no inhibition on Novozym 435. However, ethanol with concentrations above 0.08 mol L^{-1} inhibited Novozym 435 following the uncompetitive inhibition pattern. The kinetic constants were obtained subsequently through non-linear regression analysis, and the fitted parameters are: V_{max} 1.29 mmol min^{-1} g^{-1}, K_m 0.06 mol L^{-1}, K_i 0.37 mol L^{-1}. From the established kinetic equation, the simulated data of initial rate coincided with the experimental data.

Acknowledgments

This work was supported by the Major Basic Research Development Program of China (no. 2007CB714306) and the Natural Scientific Foundation of Zhejiang (no. Z4090612).

References

[1] E.E. Jacobsen, B.H. Hoff, A.R. Moen, T. Anthonsen, J. Mol. Catal. B: Enzyme 21 (2003) 55–58.
[2] A.S. Gopalan, C.J. Sih, Tetrahedron Lett. 25 (1984) 5235–5238.
[3] M. Müller, Angew. Chem. Int. Ed. 44 (2005) 362–365.
[4] S.H. Lee, O.J. Park, Appl. Microbiol. Biotechnol. 84 (2009) 817–828.
[5] R. Öhrlein, G. Baisch, Adv. Synth. Catal. 345 (2003) 713–715.
[6] A. Liljeblad, A. Kallinen, L.T. Kanerva, Curr. Org. Synth. 6 (2009) 362–379.
[7] Y. Shapira, B. Glick, S. Harel, J.J. Vattin, A. Gutman, Pediatr. Neurol. 9 (1993) 35–38.
[8] S. Korematsu, Y. Kosugi, T. Kumamoto, S. Yamaguchi, T. Izumi, Pediatr. Neurol. 41 (2009) 151–153.
[9] A. Santoro, M.B. Lioi, J. Monfregola, S. Salzano, R. Barbieri, M.V. Ursini, Mutat. Res. 587 (2005) 16–25.
[10] R. Öhrlein, G. Baisch, N. End, H.J. Kirner, F. Bienewald, WO 03/004450, WO 03/004455, WO 03/004456, 2003.
[11] J. Monteiro, J. Braun, F. Le Goffic, Synth. Commun. 20 (1990) 315–319.
[12] A.R. Moen, B.H. Hoff, L.K. Hansen, T. Anthonsen, E.E. Jacobsen, Tetrahedron: Asymmetry 15 (2004) 1551–1554.
[13] E.M. Anderson, K.M. Larsson, O. Kirk, Biocatal. Biotransform. 16 (1998) 181–204.
[14] J. Pfeffer, M. Rusnak, C.-E. Hansen, R.B. Rhlid, R.D. Schmid, S.C. Maurer, J. Mol. Catal. B: Enzyme 45 (2007) 62–67.
[15] J.M. Palomo, M. Filice, R. Fernández-Lafuente, M. Terreni, J.M. Guisán, Adv. Synth. Catal. 349 (2007) 1969–1976.
[16] D.S. Rodrigues, A.A. Mendes1, M. Filice, R. Fernández-Lafuente, J.M. Guisán, J.M. Palomo, J. Mol. Catal. B: Enzyme 58 (2009) 36–40.
[17] Z. Cabrera, G. Fernández-Lorente, R. Fernández-Lafuente, J.M. Palomo, J.M. Guisán, J. Mol. Catal. B: Enzyme 57 (2009) 171–176.
[18] D.S. Rodrigues, G.P. Cavalcante, G.F. Silva, A.L.O. Ferreira, L.R.B. Goncalves, World J. Microbiol. Biotechnol. 24 (2008) 833–839.
[19] G. Yang, J.P. Wu, G. Xu, L.R. Yang, Bioresour. Technol. 100 (2009) 4311–4316.
[20] N. Miletić, R. Rohandi, Z. Vuković, A. Nastasović, K. Loos, React. Funct. Polym. 69 (2009) 68–75.
[21] H.P. Dong, Y.G. Zheng, Chromatographia 71 (2010) 85–89.
[22] J.E. Bailey, D.F. Ollis, Biochemical Engineering Fundamentals, 2nd ed., 1986, pp. 212–214.
[23] R.H. Perry, D.W. Green, J.O. Maloney, Perry's Chemical Engineer's Handbook, McGraw-Hill, New York, 1984.
[24] J.M. Palomo, G. Fernández-Lafuente, J.M. Guisán, G. Fernández-Lafuente, Adv. Synth. Catal. 349 (2007) 1119–1127.
[25] G. DeSantis, K. Wong, B. Farwell, K. Chatman, Z.L. Zhu, G. Tomlinson, H.J. Huang, X.Q. Tan, L. Bibbs, P. Chen, K. Kretz, M.J. Burk, J. Am. Chem. Soc. 125 (2003) 11476–11477.